

Article

Viscoelastic Behavior of Crude Oil-Gum Emulsions in Enhanced Oil Recovery

Mamdouh T. Ghannam ^{1,*}, Mohamed Y. E. Selim ², Abdulrazag Y. Zekri ¹ and Nabil Esmail ³

¹ Department of Chemical and Petroleum Engineering, Faculty of Engineering, United Arab Emirates University, Al-Ain P.O. Box 15551, United Arab Emirates; a.zekri@uaeu.ac.ae

² Department of Mechanical Engineering, Faculty of Engineering, United Arab Emirates University, Al-Ain P.O. Box 15551, United Arab Emirates; mohamed.selim@uaeu.ac.ae

³ Department of Mechanical Engineering, Concordia University, 1455 de Maisonneuve Boulevard W., Montreal, QC M3G 1M8, Canada; esmail@encs.concordia.ca

* Correspondence: mamdouh.ghannam@uaeu.ac.ae

Abstract: The experimental study of the Creep-recovery examination is necessary to understand the viscoelastic behavior of crude oil-Xanthan gum emulsions. The experimental measurements and analysis of these tests were completed using RheoStress RS100 under controlled stress CS-mode. Rheometers with CS-mode allow for a useful and direct technique for the experimental measurements of creep and recovery stages. This investigation covers a wide range of crude oil concentration of 0–75% by volume, Xanthan concentration range of 0–10⁴ ppm, and two types of Xanthan gums are used and investigated. The creep-recovery measurements of crude oil-Xanthan gums emulsions were extensively investigated. It was important to find the linear viscoelastic range for the examined crude oil-Xanthan gum emulsions. The experimental measurements and analysis of the creep-recovery examinations showed that the linear viscoelastic range was up to 1 Pa. The experimental investigation showed that the higher the concentration of the used gum and crude oil, the lower the compliance of the emulsions. For the Xanthan concentrations of less than 10³ ppm, the crude oil-gum emulsion exhibited viscous behavior. However, for the Xanthan concentration of higher than 10³, the examined emulsions displayed viscoelastic behavior.

Keywords: crude oil; xanthan; creep; recovery; polymer; emulsion



Citation: Ghannam, M.T.; Selim, M.Y.E.; Zekri, A.Y.; Esmail, N. Viscoelastic Behavior of Crude Oil-Gum Emulsions in Enhanced Oil Recovery. *Polymers* **2022**, *14*, 1004. <https://doi.org/10.3390/polym14051004>

Academic Editor: Michal Sedlačik

Received: 15 December 2021

Accepted: 14 January 2022

Published: 2 March 2022

Publisher's Note: MDPI stays neutral with regard to jurisdictional claims in published maps and institutional affiliations.



Copyright: © 2022 by the authors. Licensee MDPI, Basel, Switzerland. This article is an open access article distributed under the terms and conditions of the Creative Commons Attribution (CC BY) license (<https://creativecommons.org/licenses/by/4.0/>).

1. Introduction

A considerable amount of crude oil—around half of the original magnitude—cannot be produced by traditional methods. Thus, enhanced oil recovery (EOR) is a very effective approach to extract the retained oil in an oil well [1]. There are many techniques that can be utilized to achieve this goal; some of these methods are alkali and surfactants as reported by Wylde et al. (2013) [2], and carbon dioxide injection [3,4]. Arjmand et al. (2012), Wang et al. (2013) and Wei et al. (2018) reported that the injection of polymer solution into oil wells is one of the effective techniques to capture a significant amount of the trapped oil in place [5–7]. Polymers can be used to modify the rheological properties of the pumped solutions to increase mobility ratio and therefore the crude production rate [8]. Polymer injection into crude oil wells is a useful technique of cultivating more crude oil through increasing the viscosity of the solution [9].

Polysaccharide biopolymer is one of the polymers that are widely employed in polymer flooding. Xanthan gum is a high molecular weight polysaccharide, which plays an important role in essential industries such as food and pharmaceutical [10]. Kamal et al. (2015) and Agi et al. (2018) revealed that many biopolymers may be injected in an oil well, whereas the Xanthan option is the highest utilized biopolymer. Xanthan gum is stable at high temperature and salinity, in-expensive, non-toxic, and biodegradable [11,12]. Therefore, Xanthan gum provides many attractive characteristics such as forming aqueous

solution of high viscosity even for low gum concentration and chemically stable to function at well conditions [13]. Xanthan gum has been investigated by chemical and physical studies [14,15]. Rodd et al. (2000) reported that the aqueous solutions of Xanthan gum are widely studied for its flow behavior characteristics [16]. Xanthan solutions exhibit strong pseudoplastic behavior with significant suspending properties, which improve Xanthan characteristics for different applications such as nutrition, outlooks, medications and crude oil industries [16,17]. Whistler and BeMiller (1997) reported that the Xanthan gum aqueous solutions showed strong pseudoplasticity behavior which resulted from the development of high molecular weight collections of rigid molecules [18]. The Xanthan molecules in the well-arranged structure would reinforce the polysaccharide solution [19]. Sato et al. (1984) found that the polysaccharide molecules perform as a stiff shape at lower molecular weight, while at higher molecular weight the molecules modify to wormlike coils [20].

To reveal the viscoelastic properties of emulsions consists of crude oil and Xanthan material, creep-recovery investigation is one of the very useful techniques that can be employed. This test allows us to study the deformation response of a sample when a constant stress is applied versus elapsed period, as explained by Ferry (1980). Examined materials that exhibit viscoelastic behavior are comprised of stretched chain molecules, which mix and coil together to form a complex structure at a low energy level [21]. Through the distortion phase, these molecules elongate and increase the connection direction angles with an increase in the energy level. Li et al. (2002) described the recovery phase when the applied stress is released; the molecules of the examined sample attempt to regain their previous configuration and energy level [22].

Viscoelasticity is the property of constituents that display both viscous and elastic appearances through the deformation stage, exhibiting time-dependent strain. For materials that show only elastic behavior, the extent of distortion is relative to the assigned stress and this magnitude of deformation is sustained if the assigned stress is maintained. After the assigned stress is freed, the present distortion vanishes concurrently as elaborated upon by Ferry (1980) and mentioned by Li et al. (2002) [21,22]. Therefore, elasticity results from the bond extending as a response to the applied stress on an ordered solid structure, whereas viscosity results from the molecular dissemination inside liquid materials due to the effect of the applied shear stress. Dolz et al. (2008) studied the creep and recovery of oil food emulsions with viscoelastic behaviors [23]. They found that all the examined emulsions of their study were characterized by viscous and elastic contours. For materials with viscoelastic activities, the structure experiences distortion within the network restrictions. Then unceasing distortion leads to linkage disassembling. When the assigned stress is freed, the distortion involved both the retained viscous portion and a regained elastic contribution [24].

The viscoelastic behavior of crude oil-Xanthan emulsions is vital for many engineering applications such as in the crude oil industries. The intention of the existing study is to explore the viscous and elastic behaviors for crude oil-gum emulsions. This experimental assessment addresses different crude oil and gum concentrations of two types of Xanthan gums.

2. Materials and Methods

2.1. Xanthan Materials

Two Xanthan gums were used for this study. The first one is a chemical grade from Sigma-Aldrich Canada Ltd. (Oakville, ON L6H 6J8, Canada), product # G1253 under the product name of Sigma. The second type is an industrial grade of Xanthan gum from CP Kelco (Atlanta, GA 30339, USA) with product # 10040282, and product name of Kelzan. Both gums are white to tan colored powders, and they are recommended to be used for non-food applications such as a thickener and rheology control agents.

2.2. Crude Oil

Crude oil from the North Sea was employed in all the experimental measurements with a viscosity of 7.16 mPas at 40 °C, a density of 880.6 kg/m³ at 15 °C, and an acid value of 0.0012 kg KOH/kg. The crude oil was supplied by Shell Canada Limited.

2.3. Emulsifying Agent

A surfactant material is necessary to prepare stable oil emulsions. It is commonly added into an oil-aqueous phase system as an emulsifying agent to lower the interfacial tension between the oil phase and the aqueous solution medium, and to stabilize the presence of the oil droplets within the aqueous continuous phase [25]. Triton X-100 from Sigma-Aldrich Canada Ltd. was used as a surfactant with a specific gravity of 1.07 and flash point of 113 °C.

2.4. Preparation of Crude Oil-Xanthan Emulsions

The Xanthan solutions were prepared first by mixing the Xanthan gum powder slowly in 0.25 L of warm distilled water to the required concentration. The solutions were gently stirred until all the Xanthan gum completely dissolved. Since the Xanthan solution is biodegradable, 1.0 gm formaldehyde was added and the solutions were stored at 4 °C until use to avoid bacterial growth [26,27]. Crude oil-Xanthan gum emulsions were obtained by well mixing of crude oil and Xanthan gum aqueous solution which contains 1 wt. % of Triton X-100 as a surfactant material. A Silent Crusher M homogenizer (Heidolph Instruments GmbH and Co, Schwabach, Germany) was used at a speed of 10⁴ rpm for 5 min to prepare stable crude oil-Xanthan gum emulsions [26].

2.5. Rheometer and Measurements

The creep-recovery experimental study of crude oil-Xanthan emulsions was carried out at a room temperature of 22 °C utilizing the RheoStress RS100 under CS-mode. The software package RS100 was used for operation and measurements of the viscoelastic examination. A cone-plate sensor was employed with a cone diameter of 35 mm, cone angle of 4°, and an 0.137-mm gap at the cone tip. A water bath was connected to the rheometer to control the applied temperature of the RS100 system [27].

A test sample of 1 cm³ was located on the cone-plate sensor, and then the sensor was driven automatically to the precise position. After measurement data was accomplished, the RS100 software package was used to complete the data analysis. A wide range of shear stress of 0.1 to 10 Pa, crude oil concentration range of 0–75% by volume, Xanthan concentration range of 0–10⁴ ppm, and two types of Sigma and Kelzan Xanthan gums were tested. To ensure reliability of the experimental measurements, a selected set of experimental runs were repeated three times for the same emulsion. The measured creep-recovery phases overlay with each other within the permission level of nearly ±2.5%.

3. Modelling of Creep and Recovery Behaviors

Creep is a time-dependent deformation, γ , of viscoelastic material due to the effect of constant applied shear stress τ_0 ; some of this sheared deformation is recoverable with time after the release of the applied effect. The viscoelastic behavior of a representative material is presented in Figure 1 and characterized by two phases of creep and recovery [23,28]. In Figure 1a, it is shown that a persistent level of stress such as τ_0 is influenced immediately by the specimen and preserved for a time t_0 , whereas Figure 1b shows the creep-phase and subsequent strain recovery-phase curves for a viscoelastic specimen. In reaction to the applied effect of τ_0 , the time-dependence of creep deformation γ_C of viscoelastic behavior can be stated, as in Equation (1) in which γ_s is the immediate strain, $\gamma_d(t)$ is the delayed strain, and $\gamma_v(t)$ corresponds to the viscous contribution. For the linear viscoelastic response, the γ_s denotes the elastic contribution of the specimen, which is reversible, disappears on the elimination of the applied stress and can be displayed by γ_{elastic} . The second constituent of the creep strain is $\gamma_d(t)$, which refers to the delay elastic strain with decreasing rate over

time and requires time for the complete recovery. This contribution can be referred to the chain uncoiling [21]. The third constituent $\gamma_v(t)$ represents the viscous flow contribution of the specimen, which is an irreversible part of the strain and increases linearly with time for the linear viscoelastic materials.

$$\gamma_C(t) = \gamma_s + \gamma_d(t) + \gamma_v(t) \tag{1}$$

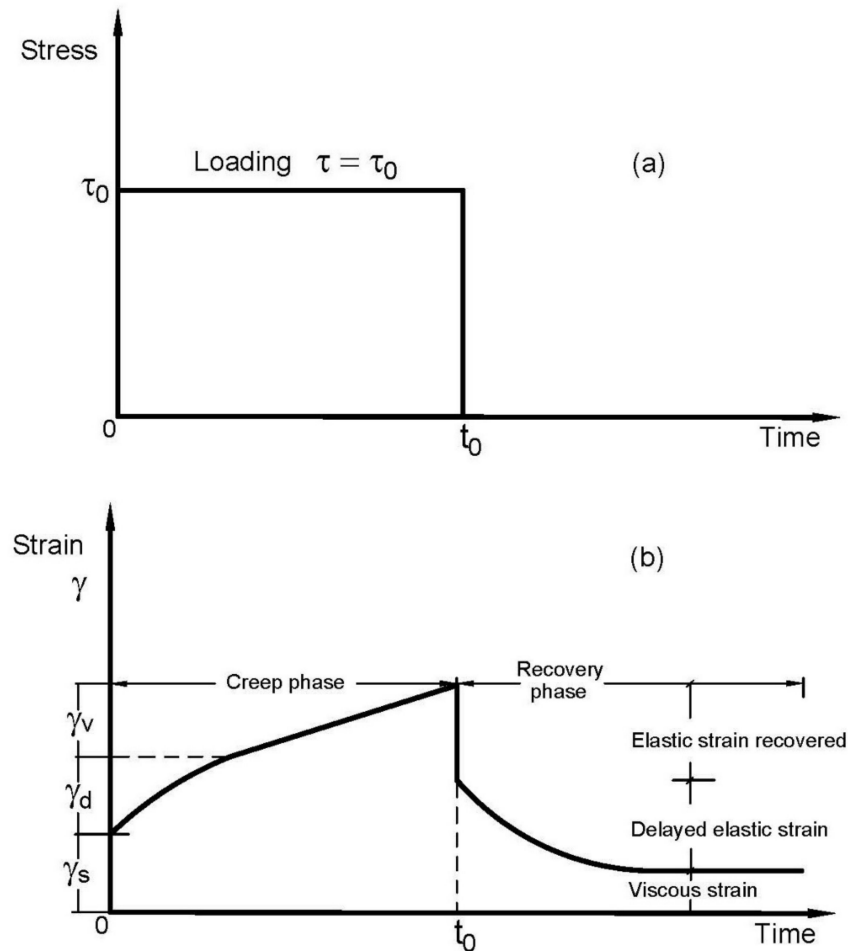


Figure 1. Viscoelastic material curve. (a) Loading mode; (b) Creep and recovery behaviors.

Under the applied constant shear stress τ_0 , materials with viscoelastic response exhibit a time-dependent deformation profile of $\gamma_C(t)$ as:

$$\gamma_C(t) = \tau_0 J_C(t) \tag{2}$$

$J_C(t)$ represents the material compliance; it exhibits the material deformation at a definite assigned stress. By introducing Equation (2) into Equation (1), the creep compliance $J_C(t)$ can be stated as:

$$J_C(t) = \gamma_C(t)/\tau_0 = J_{\text{instantaneous elastic}} + J_{\text{delay elastic}}(t) + J_{\text{viscous}}(t) \tag{3}$$

Once the stress τ_0 is released at time t_0 , the recovery phase shows an instantaneous contraction of the immediate elastic strain recovered at t_0 , followed by a period of slow recovery of the delayed elastic strain over elapsed time, whereas the viscous strain rests

unrecovered and can be stored as perpetual deformation in the specimen. Therefore, the time-dependence of strain recovery $\gamma_R(t)$ can be presented as:

$$\gamma_R(t) = \gamma_{\text{elastic}} + \gamma_{\text{slow recovery}}(t) \quad (4)$$

Correspondingly, the $J_R(t)$ can be identified as:

$$J_R(t) = \gamma_R(t)/\tau_0 = J_{\text{elastic}} + J_{\text{slow recovery}}(t) \quad (5)$$

The creep phase of the polymer solutions can be imitated through the Maxwell- or Burger-model reliant on the presence of $J_{\text{delay elastic}}(t)$ contribution within the reported behavior. The Maxwell model comprises of a coil with modulus G_0 and a dashpot with viscosity η_0 arranged in the sequence manner as in Figure 2a. The main contributions of the Maxwell equation can be presented as [24]:

$$J_C(t) = (1/G_0) + (1/\eta_0) t \quad (6)$$

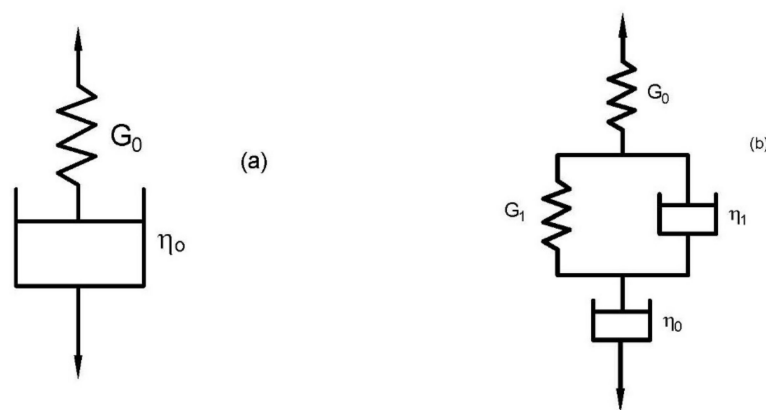


Figure 2. Maxwell and Burger models. (a) Maxwell model; (b) Burger model.

On the other hand, the Burger model involves two coils with moduli G_0 and G_1 , and two dashpots with viscosities η_0 and η_1 . This model is a series combination of the Maxwell and Kelvin–Voigt models arranged as in Figure 2b. The Burger model can be formed by the following mathematical model [24]:

$$J_C(t) = (1/G_0) + (1/\eta_0) t + (1/G_1) (1 - \exp(-t/\lambda_1)) \quad (7)$$

4. Results and Discussion

4.1. Flow Behavior of Oil-Xanthan Emulsions

The flow behavior of crude oil-Xanthan emulsions was explored in relations of viscosity and shear stress versus shear rate [27]. It has been reported that the flow behaviors of these emulsions rely upon the shear rate, kind of the added gum, and concentration of the added crude oil and gum. The Xanthan solutions of both tested types showed non-Newtonian with shear thinning profile in which the apparent viscosity diminished with shear rate. Similar flow behaviors were reported by Yeon et al. (2014) and Khan et al. (2018) [29,30]. The flow manner of crude oil-Xanthan mixture is characterized by non-Newtonian with shear thinning response [16–18]. The measured viscosity of the examined emulsions revealed that the flow behavior relies primarily on the shear rate and Xanthan gum addition. Jha et al. (2018 and 2021) studied the effect of polymers on the rheological properties of oil-water emulsions, and the impact of Xanthan gum on the development emulsion drilling fluids with strong shear thinning behavior were concluded [31,32]. The impact of gum addition is more manifest at the lower range of shear rate. Nevertheless, at greater shear rate the hydrodynamic result is more dominant than the gum concentration.

In addition, it has been found that the Casson model, Equation (8), can be used to fit the reported measurements of the investigated emulsions over the examined concentration range [27].

$$\tau = \left(\tau_{\text{app}}^{0.5} + (\dot{\gamma}\eta_c)^{0.5} \right)^2 \quad (8)$$

where τ is the shear stress in Pa, τ_{app} is the apparent yield stress in Pa, $\dot{\gamma}$ is the shear rate in s^{-1} , and η_c is the apparent viscosity in Pa.s. The apparent viscosities of the crude oil-Xanthan emulsions are higher than their corresponding solutions. For the lighter concentration of crude oil ($\leq 25\%$) and gum addition (≤ 1000 ppm), both kinds of gum emulsions showed comparable viscosity profiles. However, for the higher concentrations of crude oil and gum, the Kelzan emulsions exhibited slightly higher viscosity profiles than the Sigma emulsions [27].

4.2. Linear Viscoelastic Range of the Examined Emulsions

When a tested sample with viscoelastic behavior is exposed to constant shear stress of τ_0 , the emulsion reveals time-dependent strain behavior with compliance responses as displayed by Equation (2). The higher the values of the emulsion compliance display, the easier the liquid can be strained. The behavior of the emulsion compliance depends upon the level of the applied shear stress. At the lower values of the applied shear stress, the viscoelastic material usually shows a rectilinear profile. However, for the higher shear stresses, the viscoelastic profile exhibits a non-linear behavior in which the test results rely on the settings and considerations of the instrument [33]. Moreover, within the linear limits, the applied shear stress will not be destructive, and the distorted consequences can be recalled if the assigned shear is removed, which reveals that the sample structure was elastically stressed while the structure remained undamaged. Consequently, inside the linear limits, the compliance behavior will not rely on the assigned shear [33].

It is necessary to find the shear stress range which results in linear viscoelastic behavior for the crude oil-gum emulsions. The following test was carried out for different assigned shear stresses, gradually ascending in order to find the linear limitations. Firstly, the emulsion sample was placed in the right position inside the RS100 unit; then, a constant shear stress of a low value of 0.1 Pa is applied for a period of 250 s to check the creep phase. The assigned shear is then removed to follow the recovery profile for another period of 250 s. Similar examining tests were repeated for new emulsion samples of the same characteristics, but at higher applied shear stresses. Variety of shear stresses over the range of 0.1–10 Pa were applied. If the compliance results of various assigned shear stresses overlapped each other, this provided the linear viscoelastic range. On the opposite side, the non-linear domain caused the compliance profiles to diverge considerably from the linear profiles [33,34].

Many experimental runs have been completed for different emulsions with different applied shear stresses to determine the stress range that establishes the linear viscoelastic range. Figure 3a,b shows typical examples of these tests for 25% and 50% crude oil in the presence of Sigma and Kelzan gum. These investigations of the creep-recovery behaviors under different assigned shear stresses up to 10 Pa in Figure 3a,b show that the assigned stresses up to 1.0 Pa cause linear profiles for the whole tested crude oil-Xanthan emulsions. Dolz et al. (2008) studied the linear viscoelastic region of some oil-Xanthan emulsions by using the stress sweep between 0.1 and 100 Pa, and they recorded the creep tests at a constant stress amplitude of 3 Pa for emulsions [23]. However, Pal (1996) carried out creep-recovery tests for polymer thickened oil-water emulsions at a constant stress amplitude of ≤ 0.5 Pa [35]. Thus, unless it is cited otherwise, all the further experimental runs of viscoelastic behavior are tested at an assigned stress of 0.1 Pa to confirm that the structure of the emulsions can be elastically strained, whereas the sample structure remains unbroken [34].

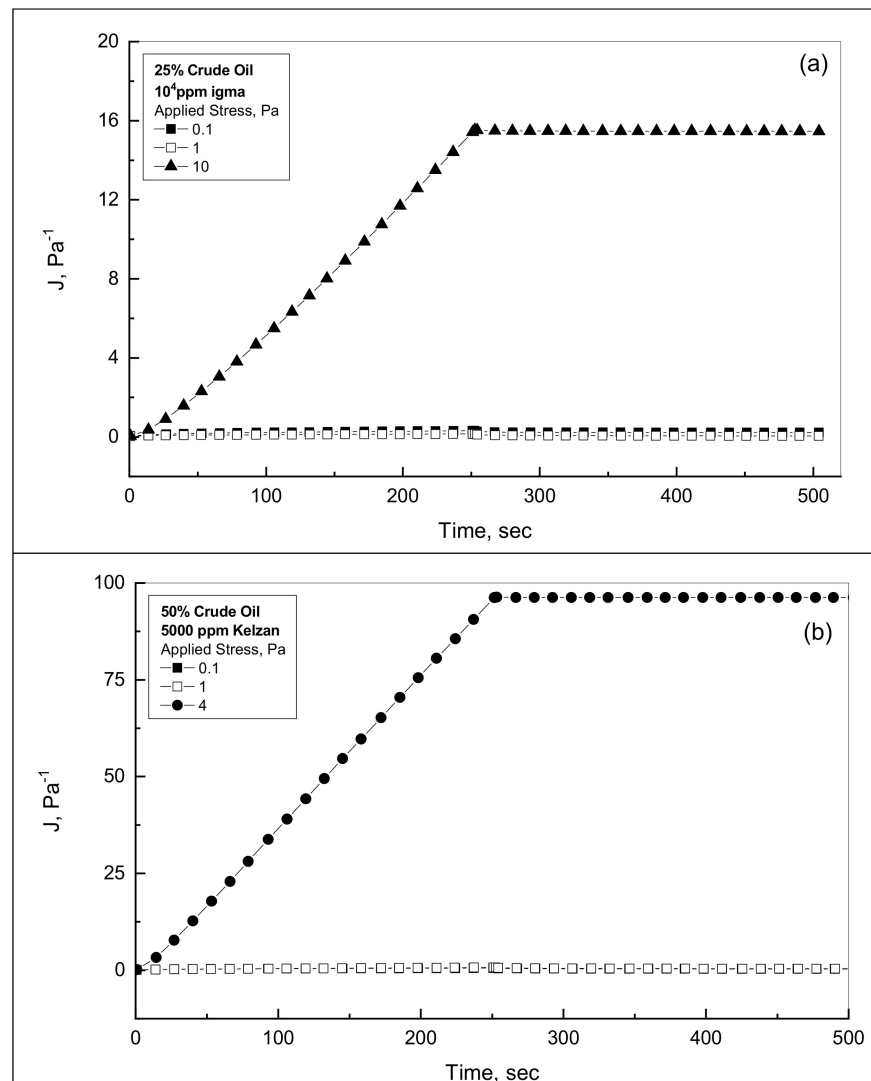


Figure 3. Compliance behavior for two different emulsions. (a) 25% oil-10⁴ ppm Sigma emulsion; (b) 50% oil-5000 ppm Kelzan emulsion.

4.3. Effect of Xanthan Concentration

To address the effect of the gum addition on the viscoelastic performance in terms of creep and recovery of the prepared emulsions, a wide range of Sigma addition over the range 0–10⁴ ppm was tested for different oil emulsions. Figure 4a,b displays typical examples for the examined emulsions in terms of compliance against time. As can be observed from Figure 4a,b, the Sigma addition commands the performance and the magnitude of the crude oil-Xanthan results. The higher the addition of the tested gum, the lower the compliance results of the emulsion. For each emulsion, if the assigned constant shear stress is applied, the compliance measurement of Sigma emulsions increases gradually with time within the creep phase. This behavior reached its peak at the end of the creep phase, i.e., at the end of 250 s. Within the creep phase, the time rate of compliance change decreased over the elapsed time. This behavior can be explained through the tested emulsion, which experienced an increase in creep resistance. Therefore, the deformation of the tested emulsion became more difficult as the material was stressed [22,23,33].

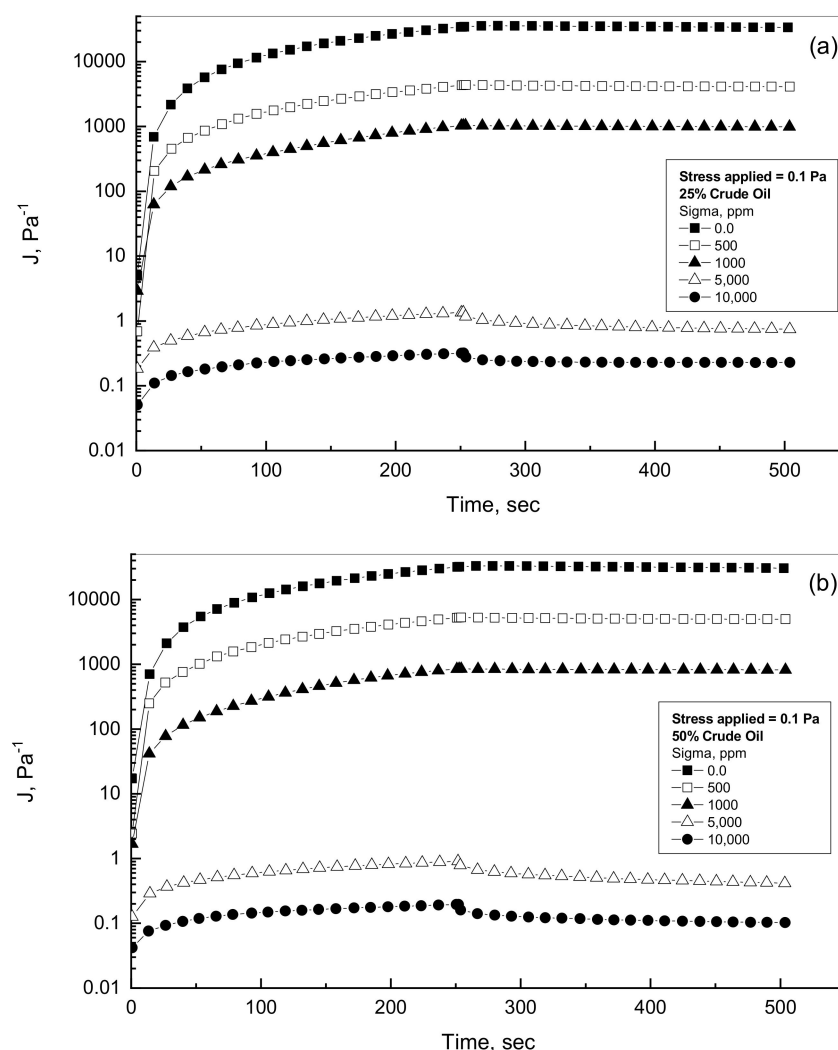


Figure 4. Creep-recovery behavior for 25% and 50% crude oil-Sigma emulsions. (a) 25% oil-Sigma emulsions; (b) 50% oil-Sigma emulsions.

Once the creep mode was completed at the end of 250 s, the allocated shear stress was removed, and the recovery phase was observed versus elapsed period for the subsequent 250 s, as can be assessed in Figure 4. Table 1 shows the compliance measurements at the end of creep phase J_{250} , and at the end of recovery phase, J_{500} , for the 25% and 50% crude oil-Sigma gum emulsions. As listed in Table 1, the compliance values decline significantly with the addition of gum and crude oil concentrations. These remarks are in a full agreement with the results reported by Pal (1996) in which the polymer and crude oil concentrations dictate the viscoelastic behavior in terms of creep and recovery [35]. The addition of crude oil into the polymer emulsions leads to lower creep-recovery behavior and consequently higher elastic response [35].

Table 1. Compliance measurements at the end of creep and recovery modes.

Sigma, ppm	25% Oil		50% Oil	
	J_{250}, Pa^{-1}	J_{500}, Pa^{-1}	J_{250}, Pa^{-1}	J_{500}, Pa^{-1}
0	34,221	33,571	31,848	30,433
500	4304	4107	5211	4953
1000	1026	989	848	818
5000	1.351	0.748	0.91	0.417
10,000	0.318	0.229	0.195	0.103

As discussed earlier, it is necessary to address the recovery achieved by the emulsion at the end of each test. The compliance measurements can be utilized to anticipate the magnitude of the recovery that can be sustained by using Equation (9) taking into consideration the differences between the reported values of deformation at the creep end and the deformation at the recovery end w.r.t. the deformation at the end of the creep phase [23]. Figure 5 illustrates the recovery percentage versus the Sigma concentration for two crude oil concentrations of 25% and 50%. In general, the recovery% enhances gradually with both the crude oil and gum concentrations up to 5000 ppm. The recovery % of the tested emulsions reveals the elastic contribution of the oil-gum emulsion. Figure 5 shows that the oil-gum emulsions with gum addition of up to 1000 ppm display only viscous behavior since the recovery % is very near zero. The recovery % of the higher concentrations of both gum and oil exhibits greater recovery, which indicates viscoelastic behavior. Therefore, the presence of polymer material and crude oil boosts the elastic contribution of the tested emulsions as reported by Pal (1996) [35].

$$\text{Recovery\%} = (\text{Creep end value} - \text{Recovery end value}) \times 100 / \text{Creep end value} \quad (9)$$

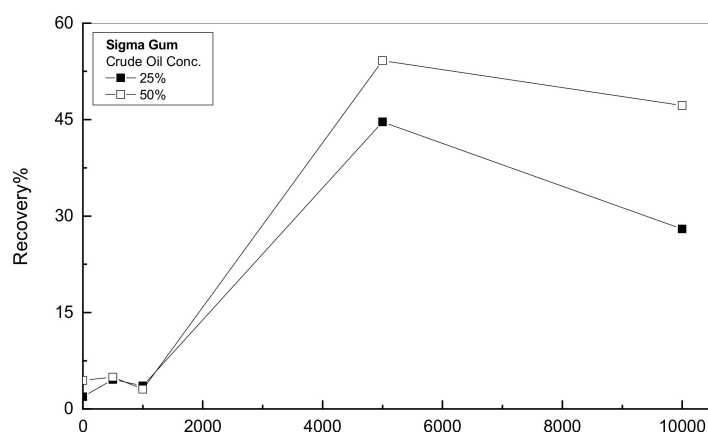


Figure 5. Recovery behavior for crude oil-Sigma emulsions.

4.4. Effect of Crude Oil Concentration

The aim of this investigation is to search for the role of oil presence within the emulsion in viscous and viscoelastic diverse situations. Figure 6a illustrates the creep and recovery behaviors for the 0, 25%, and 75% of oil addition into 500 ppm solution as a typical example for low Sigma gum concentration. Figure 6a shows viscous performance for the 500-ppm solution, i.e., without crude oil. For this case, the compliance value reaches 5650 Pa⁻¹ at the end of creep phase of 250 s. The availability of crude oil inside the Sigma gum solution progressively decreases the measured compliance values. For example, the compliance value at the end of the creep phase reaches 4305 and 1362 Pa⁻¹ for 25% and 75% oil addition. Both of these examined emulsions exhibit recovery % of less than 5% at the end of the recovery phase. Therefore, the three tested cases of the 500-ppm gum solution and its emulsions of 25 and 75% crude oil addition display only viscous behavior since the reported recovery % is very limited. Pal (1996) concluded only viscous behavior for oil-polymer emulsions with an oil concentration of less than 65% by volume [35].

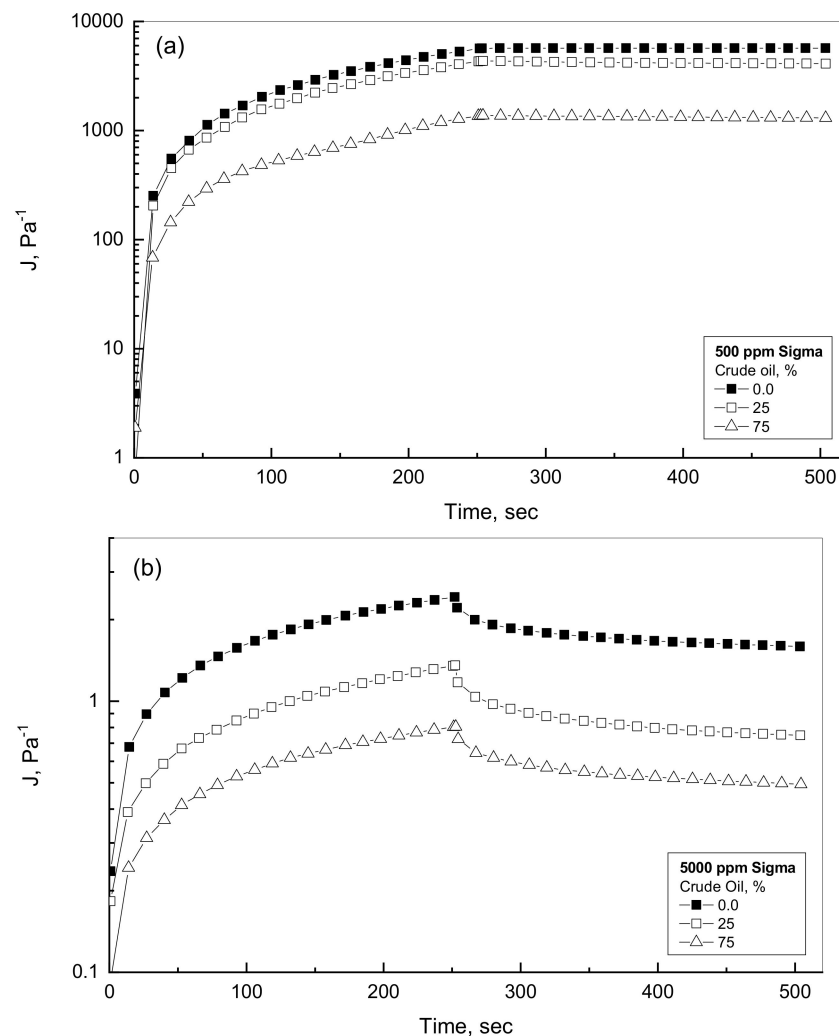


Figure 6. Effect of oil addition for 500 and 5000 ppm of Sigma emulsions. (a) Low Sigma concentration; (b) High Sigma concentration.

It is necessary to examine the similar profiles for the higher Sigma gum concentration. Figure 6b, for the 5000 ppm Sigma solution, illustrates the viscoelastic behavior of the gum solution and two more crude oil-Sigma emulsions. These tested cases of high gum concentration demonstrate much lower values of the measured compliance associated with higher elastic recovery portion in comparison with the viscous environment case displayed in Figure 6a. The existence of oil regularly depresses the compliance results and slightly surges the recovery contribution. For example, the measured compliance values at the end of creep phase are 2.424, 1.351 and 0.803 Pa^{-1} for 0, 25% and 75% oil content, as can be observed in Figure 6b. The recovery % according to Equation (9) for 0, 25% and 75% emulsions are 34.3%, 44.6% and 38.5%, respectively. Therefore, the addition of crude oil into higher gum concentration of 5000 ppm enhances the elastic activities of the crude oil-Sigma gum emulsions. The existence of crude oil droplets phase within the aqueous phase of the Xanthan gum enhances the apparent viscosity of the emulsions, which can be contributed to the interactions and collisions between the oil droplets and the polymer network [27]. The viscoelastic behavior of the examined emulsions is in agreement with the characteristics of the flow profile discussed earlier, owing to the presence of oil phase. Sosa-Herrera et al. (2008) reported that the elastic response of emulsion is higher than that of the polymer solution, which is due to the presence of suspended oil droplets within the polymer solution [36,37].

The surface charges of the polysaccharide molecules allow for the interconnection between the oil surface and the molecules of the Xanthan gum [38]. Thus, an interfacial film establishes through either hydrogen bonds, van der Waals or electrostatic interactions, providing oil-gum stabilized emulsion [39,40]. Numerous studies have specified that the hydrogen bonding and electrostatic interactions display a significant effect on the oil-gum network structure [41]. Jiang et al. (2020) reported that the hydrogen bonding and electrostatic interactions of the oil-gum emulsion form pseudoplastic fluids with oil elastic behavior [42]. Therefore, the viscoelastic response of the crude oil-gum emulsions can be attributed to the viscoelasticity behavior of the high concentration gum solution continuous phase, which is a viscoelastic in nature, the droplets dispersed phase of the high concentration of the crude oil which exhibits some shape elasticity, and the intermolecular interactions between the oil droplets dispersed phase and the polymer networks structure.

4.5. Comparison of Sigma and Kelzan Creep-Recovery Behavior

It is valuable to investigate the viscoelastic characteristics of oil-gum mixtures in the presence of two different gums such as Kelzan and Sigma. This study observed variety of selected additions of oil and gum. Figure 7a,b shows the compliance profiles for low- and high-additions of Sigma and Kelzan in the presence of little concentration of 25% crude. Figure 7a displays almost linear behavior for both of creep and recovery phases for the low gum concentration of up to 1000 ppm with Sigma emulsions considerably higher profiles than the Kelzan emulsions. For the low gum concentration of up to 1000 ppm, Figure 7a reveals very low recovery % by using the compliance results at the expiration of both creep and recovery phases. This kind of creep-recovery profile for the low gum concentrations can be considered viscous behavior as discussed before [36,43]. Figure 7b shows the creep-recovery behavior for the higher gum concentration range in the existence of 25% crude oil. As can be described from Figure 7b, much less compliance values with non-linear profiles for both creep and recovery phases reveal viscoelastic characteristics for both tested Xanthan gums. This observation can be referred to the viscoelasticity nature of the high gum concentrations, the crude oil dispersed phase and the intermolecular interactions of the oil droplets medium inside the Xanthan gum network formed by the high concentration. This means that the elastic characteristic improves considerably with further addition of the Xanthan gum, leading to the formation of gel-like behavior [36,43]. Similar behaviors are observed in Figure 8a,b for the low- and high-Xanthan gum additions in the presence of 75% crude oil concentration.

The recovery % analysis was completed for the examined oil-gum emulsions with various additions of Sigma and Kelzan. Figure 9 exhibits the analysis of the recovery % versus the gum concentration for the two tested Sigma and Kelzan. In general, for gum concentration higher than 1000 ppm, the recovery % increases considerably with gum addition and oil concentration. One exception for this behavior is the 25% crude oil-Sigma emulsion of 10^4 ppm concentration; it shows a slight drop in recovery % from its peak at 5000 ppm. Figure 9a,b show that the Kelzan emulsions display higher recovery % than the Sigma emulsions. The recovery % of the examined emulsions depicts the elastic portion within the crude oil-gum emulsions. It is obvious from Figure 9 that the lower concentrations than 1000 ppm of both types of gums emulsions can be considered only viscous behavior since their recovery % is very close to zero for both materials. This conclusion is in agreement with the results reported by the Akiyama et al. (2005) [43]. The presence of high polymer concentration within oil emulsion forms some kind of gel status through the associated networks of polymer molecules during the intermolecular interactions [44]. However, for the diluted polymer solutions, the connected network will not be available. Therefore, the higher concentrations of Xanthan gums emulsions show much higher recovery %, which indicates viscoelastic behavior [45].

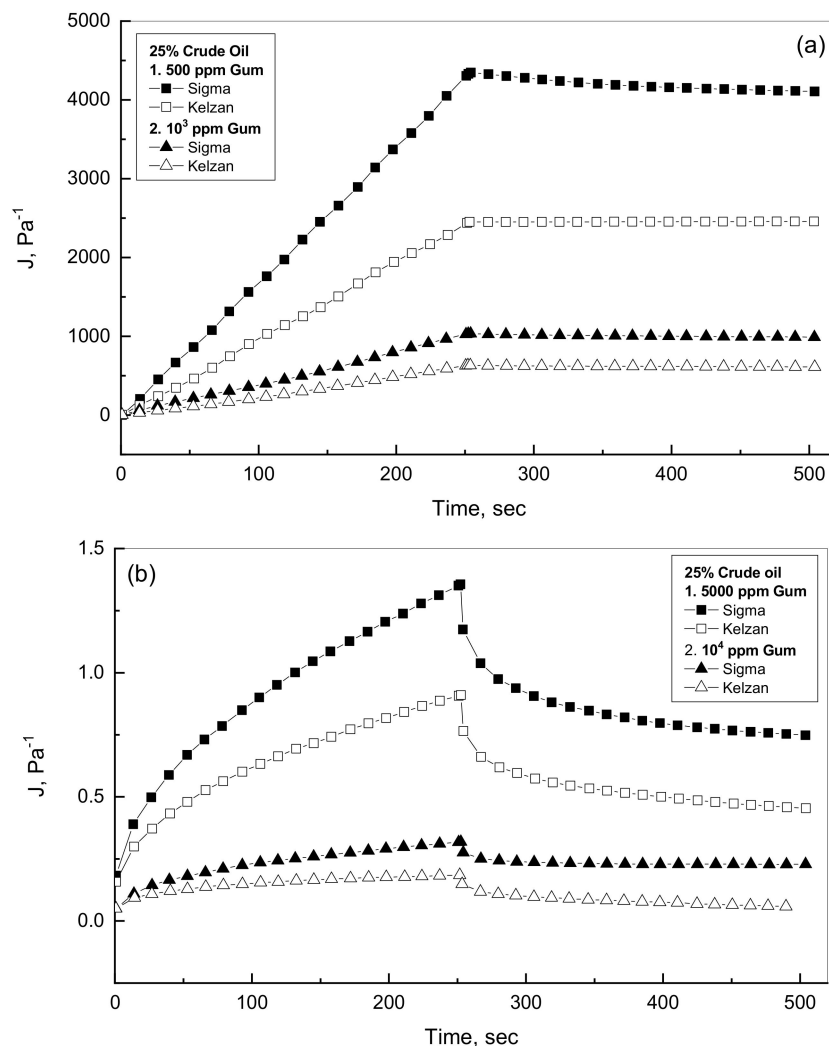


Figure 7. Creep-recovery behavior of Sigma and Kelzan for 25% oil emulsions. (a) Low Xanthan concentration; (b) High Xanthan concentration.

From the earlier discussion and illustrations of the creep behavior, it is obvious that the oil-gum mixtures of light Xanthan content (i.e., less than 5000 ppm) perform in almost full viscous behavior and will be modelled by Equation (6). Whereas the higher gum concentrations of the oil emulsions exhibit instantaneous-, delayed elastic-, and viscous flow-deformations of viscoelastic behavior. Consequently, these higher gum concentrations of oil emulsions can be demonstrated sufficiently with Equation (7). Additionally, these remarks can be acquired from the examination of the Maxwell- and Burger-models. The outcomes of these models are listed in Tables 2 and 3 with the regression coefficient R^2 . Table 2 displays the Maxwell factors of G_0 and η_0 for lower concentrations of Xanthan gums with variety of crude oil addition, while the next table reports the Burger factors of G_0 , G_1 , η_0 , and η_1 for the higher Xanthan additions in the presence of diverse oil content. Table 2 shows the dashpot contribution of the viscosity η_0 values and almost a nonexistence of the coil involvement of the Maxwell model except for the 75% oil- 10^3 ppm emulsion, which displays a very minor contribution of the G_0 . Therefore, the selection and estimates of the Maxwell model support the acquired remarks of the complete viscous behavior of the lower gum emulsions of less than 5000 ppm Xanthan concentrations.

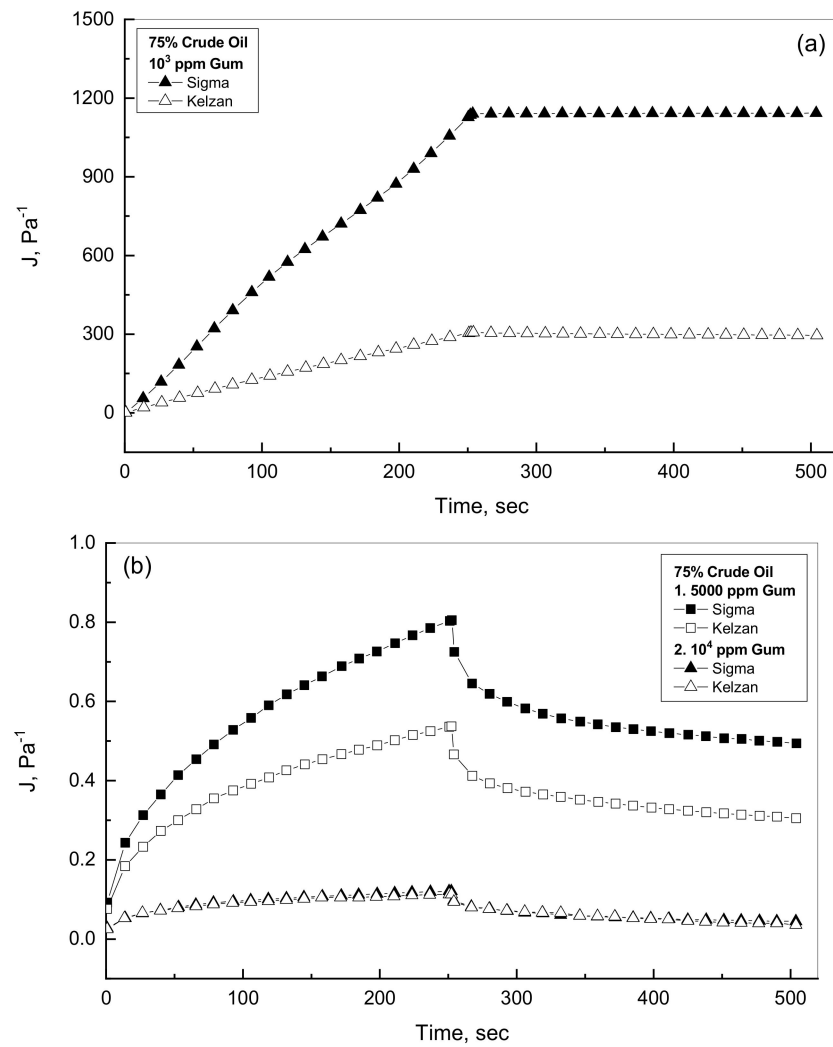


Figure 8. Creep-recovery behavior of Sigma and Kelzan for 75% oil emulsions. (a) Low gum concentration; (b) High gum concentration.

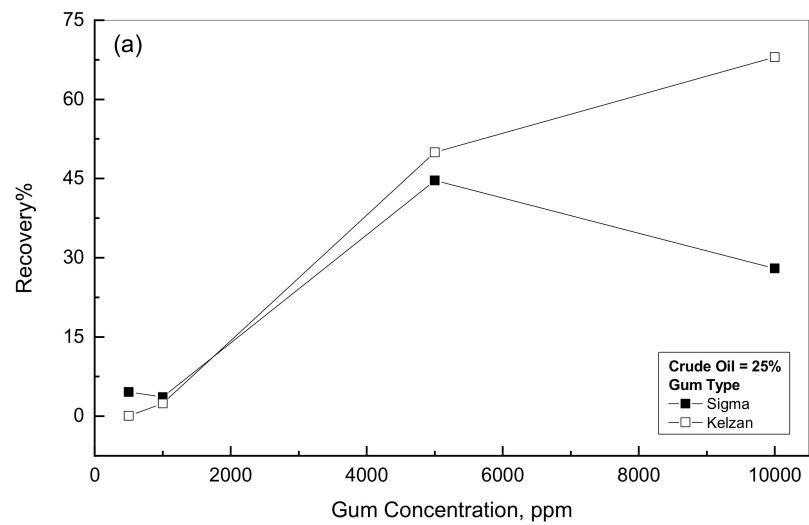


Figure 9. Cont.

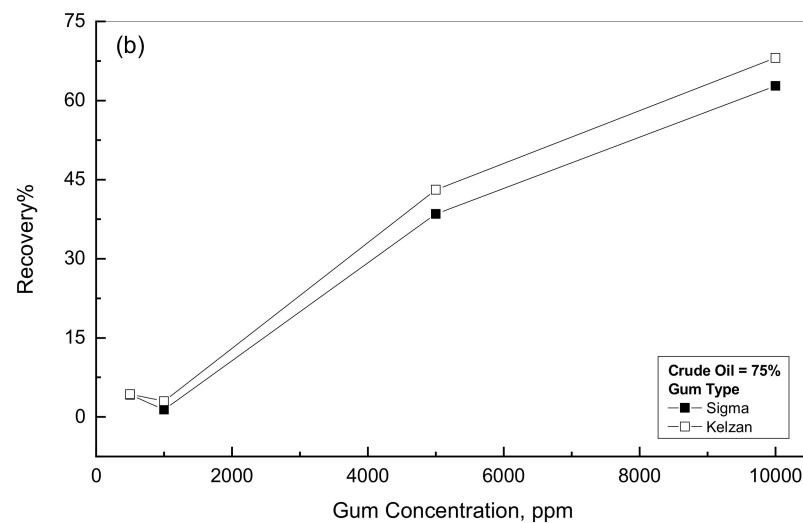


Figure 9. Recovery behavior for 25% and 75% crude oil-gum emulsions. (a) Low crude oil concentration; (b) High crude oil concentration.

Table 2. Creep modelling using Maxwell equation for lower gum emulsions.

<i>A-Sigma Xanthan</i>									
Gum Conc.	25% Oil			50% Oil			75% Oil		
	G_o	η_o	R^2	G_o	η_o	R^2	G_o	η_o	R^2
	Pa	Pas		Pa	Pas		Pa	Pas	
500 ppm	0.0	0.058	0.99	0.0	0.048	0.99	0.0	0.188	0.99
10^3 ppm	0.0	0.245	0.99	0.0	0.288	0.99	0.045	0.227	0.99
<i>B-Kelzan Xanthan</i>									
Gum Conc.	25% Oil			75% Oil					
	G_o	η_o	R^2	G_o	η_o	R^2			
	Pa	Pas		Pa	Pas				
500 ppm	0.0	0.102	0.99	0.0	0.059	0.99			
10^3 ppm	0.0	0.393	0.99	0.089	0.845	0.99			

Table 3 displays the viscoelastic modelling parameters which enhance considerably with the concentration, i.e., the viscoelastic characteristics growth significantly with emulsion concentrations of crude oil and gum additions. In general, owing to the presence of the elastic contributions of G_o and G_1 listed in Table 3; therefore, the expectation of the Burger model agrees very well with the prior remarks of the viscoelastic profiles of the higher gum and oil emulsions. For all the tested emulsions, the four parameters of the Burger model presented similar trend with oil and gum concentrations. The elastic moduli G_o and G_1 of the Burger model increase significantly with concentrations of both phases in which G_o is higher than G_1 . Therefore, the values of the instantaneous elastic modulus (G_o) are higher than the predicted values of the retarded elastic region (G_1) for all the tested emulsions.

Table 3. Creep modelling using Burger equation for higher gum emulsions.

		G_0	η_0	G_1	η_1	R^2
		Pa	Pas	Pa	Pas	
Gum Conc.		<i>A. 25% Crude Oil</i>				
5000	Sigma	5.3	333.3	2.4	83.2	0.999
10^4	Sigma	19.8	1666.7	7.8	240.0	0.999
Gum Conc.		<i>B. 50% Crude Oil</i>				
5000	Sigma	7.8	526.3	3.3	103.6	0.998
10^4	Sigma	23.8	3333.3	12.5	426.2	0.999
Gum Conc.		<i>C. 75% Crude Oil</i>				
5000	Sigma	10.2	625	3.2	117.7	0.998
10^4	Sigma	36.2	5000	17.9	537.2	0.999
Gum Conc.		<i>D. 25% Crude Oil</i>				
5000	Kelzan	6.3	555.6	3.4	117.5	0.999
10^4	Kelzan	19.7	5000	12.1	333	0.995
Gum Conc.		<i>E. 75% Crude Oil</i>				
5000	Kelzan	5.2	666.7	114.9	0.012	0.910
10^4	Kelzan	39.7	10,000	17.9	470.0	0.994

The recovery segment was observed when the applied stress τ_0 is removed at time 250 s and then the recovery phase was recorded over the period 250–500 s. The recovery phase of the viscoelastic crude oil-gum emulsions displays a sudden shrinkage of the instant elastic strain recovered at 250 s and corresponds to the Maxwell model coil modulus (G_0). The second part of recovery is slower, and gradual recapture of the deferred elastic strain with time. This gradual exponential recovery corresponds to the Kelvin–Voigt modulus (G_1). The third part of recovery is the viscous contribution which lasts unrecaptured and dissipated within the specimen [21]. Consequently, the time-dependence of $J_R(t)$ can be displayed by Equation (10) as:

$$J_R(t) = (1/G_0) + (1/G_1) \exp(-t/\lambda_1) \quad (10)$$

The modelling investigation utilizing Equation (10) was implemented to find the appropriate parameters to describe the recovery segment of the various crude oil-gum emulsions. The outcomes of this examination are listed in Table 4 and are associated with the regression factor of R^2 . Table 4 shows that the modelling parameters of Equation (10) grow gradually with further addition of both crude oil and gum materials, enhancing the recovery % behaviors of the crude oil-gum emulsions as indicated earlier in Figure 9. For all the examined emulsions, Table 4 displays that the instantaneous elastic recovery of G_0 is much higher than the gradual recovery contribution.

Table 4. Results of recovery analysis using Equation (10) for higher gum emulsions.

	<i>25% Crude Oil</i>				<i>75% Crude Oil</i>			
	G_0	G_1	η_1	R^2	G_0	G_1	η_1	R^2
	Pa	Pa	Pas		Pa	Pa	Pas	
5000 Sigma	1.29	0.003	0.103	0.95	1.96	0.008	0.310	0.95
10^4 Sigma	4.35	0.005	0.221	0.92	20.83	0.079	3.720	0.94
5000 Kelzan	2.08	0.004	0.141	0.93	3.13	0.016	0.677	0.93
10^4 Kelzan	14.79	0.044	2.017	0.92	28.25	1.118	106.45	0.94

5. Conclusions

This experimental study investigates the viscous and elastic behaviors of crude oil-Xanthan gum emulsions. The gum and oil concentrations dictate the characteristics of the creep-recovery curve and the magnitude of the measured compliance. The presence of the crude oil within the gum solution declines the measured compliance for both of creep and recovery behaviors. For the gum concentrations of higher than 10^3 ppm, the crude oil-gum emulsions display non-linear viscoelastic behaviors due mainly to the gum viscoelastic responses and the intermolecular interactions between the crude oil droplets and the Xanthan gum networks formed within the emulsions. Furthermore, the addition of crude oil enhances the elastic contribution of the tested emulsions. The reported creep-recovery profiles of the crude oil-Sigma emulsions are slightly higher than the emulsions of Kelzan. However, for the lower gum addition of less than 10^3 ppm, both types of gums emulsions display linear creep-recovery profiles of viscous behaviors. In general, crude oil-Kelzan emulsions demonstrate recovery % slightly higher than the crude oil-Sigma emulsions. Maxwell and Burger models were utilized to model both of the viscous and viscoelastic profiles of the tested emulsions. Although further studies are necessary to assess the viscoelastic behavior of the crude oil and gum emulsions, the remarks and measurements of the current study will be useful knowledge to utilize Xanthan gums in the enhanced oil recovery.

Author Contributions: Conceptualization, M.T.G.; formal analysis, M.T.G., M.Y.E.S. and A.Y.Z.; investigation, M.T.G., M.Y.E.S. and N.E.; resources, N.E.; supervision, A.A.Y.Z.; writing—Original draft, M.T.G. and M.Y.E.S.; writing—Review & editing, A.Y.Z. and Nabil Esmail. All authors have read and agreed to the published version of the manuscript.

Funding: This research received no external funding.

Institutional Review Board Statement: Not applicable.

Informed Consent Statement: Not applicable.

Data Availability Statement: Not applicable.

Conflicts of Interest: The authors declare no conflict of interest.

References

1. Hon, V.Y.; Kechut, N.I.; Razak, W.N.A.W. Enhanced Oil Recovery Potential of Heavy-Oil Fields in Africa. In Proceedings of the International Oil Conference and Exhibition in Mexico, Veracruz, Mexico, 27–30 June 2007.
2. Wylde, J.J.; Slayer, J.L.; Barbu, V. Polymeric and Alkali-Surfactant Polymer Enhanced Oil Recovery Chemical Treatment: Chemistry and Strategies Required After Breakthrough into the Process. In Proceedings of the SPE International Symposium on Oilfield Chemistry, The Woodlands, TX, USA, 8–10 April 2013.
3. Yuan, Q.; Sun, C.Y.; Yang, X. Recovery of Methane from Hydrate Reservoir with Gaseous Carbon Dioxide Using a Three-Dimensional Middle-Size Reactor. *Energy* **2012**, *40*, 47–58. [[CrossRef](#)]
4. Luan, Y.; Liu, B.; Hao, P.; Zhan, K.; Liu, J. Oil Displacement by Supercritical CO₂ in a Water Cut Dead-End Pore: Molecular Dynamics Simulation. *J. Pet. Sci. Eng.* **2020**, *188*, 106899. [[CrossRef](#)]
5. Arjmand, O.; Kalbasi, M.; Roostaei, A.R. Experimental Study of Chemical Flooding Using New Chemical Component to Enhance Oil Recovery. *Res. J. Appl. Sci. Eng. Technol.* **2012**, *4*, 3056–3061.
6. Wang, Z.; Le, X.; Zhang, C. The Role of Matching Relationship between Polymer Injection Parameters and Reservoirs in Enhanced Oil Recovery. *J. Pet. Sci. Eng.* **2013**, *111*, 139–143. [[CrossRef](#)]
7. Wei, P.; Pu, W.; Sun, L.; Li, D.; Ji, X. Alkyl Polyglucosides Stabilized Foam for Gas Controlling in High-Temperature and High-Salinity Environments. *J. Ind. Eng. Chem.* **2018**, *60*, 143–150. [[CrossRef](#)]
8. Wu, Y.F.; Mahmoudkhani, A.; Watson, P.; Fenderson, T.; Nair, M. Development of New Polymers with Better Performance Under Conditions of High Temperature and High Salinity. In Proceedings of the SPE EOR Conference at Oil and Gas West Asia, SPE 155653, Muscat, Oman, 16–18 April 2012.
9. Shiran, B.S.; Skauge, A. Enhanced Oil Recovery (EOR) by Combined Low Salinity Water/Polymer Flooding. *Energy Fuels* **2013**, *27*, 1223–1235. [[CrossRef](#)]
10. Speers, R.A.; Tung, M.A. Concentration and Temperature Dependence of Flow Behavior of Xanthan Gum Dispersions. *J. Food Sci.* **1986**, *51*, 96–98. [[CrossRef](#)]

11. Kamal, M.S.; Sultan, A.S.; Al-Mubaiyedh, U.A.; Hussein, I.A. Review on Polymer Flooding: Rheology, Adsorption, Stability, and Field Applications of Various Polymer Systems. *Polym. Rev.* **2015**, *55*, 491–530. [[CrossRef](#)]
12. Agi, A.; Junin, R.; Gbonhinbor, J.; Onyekonwu, M. Natural Polymer Flow Behaviour in Porous Media for Enhanced Oil Recovery Applications: A Review. *J. Petrol. Explor. Prod. Technol.* **2018**, *8*, 1349–1362. [[CrossRef](#)]
13. Moon, R.; Martini, A.; Nairn, J.; Simonsen, J.; Youngblood, J. Cellulose Nanomaterial Review: Structure, Properties and Nanocomposites. *Chem. Soc. Rev.* **2011**, *7*, 3941–3994. [[CrossRef](#)]
14. Ryles, R.G. Chemical Stability Limits of Water-Soluble Polymers Used in Oil Recovery Processes. *SPE Res. Eng.* **1988**, *3*, 23–34. [[CrossRef](#)]
15. Richardson, R.K.; Ross-Murphy, S.B. Non-Linear Viscoelasticity of Polysaccharide Solutions. 2: Xanthan Polysaccharide Solutions. *Int. J. Biol. Macromol.* **1987**, *9*, 250–256. [[CrossRef](#)]
16. Rodd, A.B.; Dunstan, D.E.; Boger, D.V. Characterization of Xanthan Gum Solutions Using Dynamic Light Scattering and Rheology. *Carbohydr. Polym.* **2000**, *42*, 159–174. [[CrossRef](#)]
17. Berth, G.; Dautzenberg, H.; Christensen, B.E.; Harding, S.E.; Rother, G.; Smidsrod, O. Static Light Scattering Studies on Xanthan in Aqueous Solutions. *Macromolecules* **1996**, *29*, 3491–3498. [[CrossRef](#)]
18. Whistler, R.L.; BeMiller, J.N. *Carbohydrate Chemistry for Food Scientists*; Eagan Press: St. Paul, MN, USA, 1997.
19. Milas, M.; Rinaudo, M. Conformation Investigation of the Bacterial Polysaccharide Xanthan. *Carbohydr. Res.* **1979**, *76*, 189–196. [[CrossRef](#)]
20. Sato, T.; Norisuye, T.; Fujita, H. Double-Stranded Helix of Xanthan: Dimensional and Hydrodynamic Properties in 0.1 M Aqueous Sodium Chloride. *Macromolecules* **1984**, *17*, 2696–2700. [[CrossRef](#)]
21. Ferry, J.D. *Viscoelastic Properties of Polymers*; Wiley: New York, NY, USA, 1980.
22. Li, W.H.; Du, H.; Chen, G.; Yeo, S.H. Experimental Investigation of Creep and Recovery Behaviors of Magnetorheological Fluids. *Mater. Sci. Eng. A* **2002**, *333*, 368–376. [[CrossRef](#)]
23. Dolz, M.; Hernández, M.J.; Delegido, J. Creep and Recovery Experimental Investigation of Low Oil Content Food Emulsions. *Food Hydrocoll.* **2008**, *22*, 421–427. [[CrossRef](#)]
24. Nielsen, L.E.; Landel, R.F. *Mechanical Properties of Polymers and Composites*; Marcel Dekker Inc.: New York, NY, USA, 1994.
25. Ghannam, M. Emulsion Flow Behavior of Crude Oil-Alcoflood Polymers. *J. Chem. Jpn.* **2003**, *36*, 35–44. [[CrossRef](#)]
26. Makri, E.A.; Doxastakis, G.I. Study of Emulsions Stabilized with Phaseolus Vulgaris or Phaseolus Coccineus with the Addition of Arabic Gum, Locust Bean Gum and Xanthan Gum. *Food Hydrocoll.* **2006**, *20*, 1141–1152. [[CrossRef](#)]
27. Ghannam, M.T.; Abu-Jdayil, B.; Esmail, N. Experimental Investigation of Crude Oil-Xanthan Emulsions Flow Behavior. *J. Pet. Sci. Res.* **2014**, *3*, 1–15. [[CrossRef](#)]
28. Korhonen, M.; Lehtonen, J.; Hellen, L.; Hirvonen, J.; Yliruusi, J. Rheological Properties of Three Component Creams Containing Sorbitan Monoesters as Surfactants. *Int. J. Pharm.* **2002**, *247*, 103–114. [[CrossRef](#)]
29. Yeon, H.; Zhang, K.; Hyun, B.; Jin, H. Enhanced Oil Recovery Performance and Viscosity Characteristics of Polysaccharide Xanthan Gum Solution. *Ind. Eng. Chem. J.* **2014**, *21*, 741–745.
30. Khan, S.Y.; Yusuf, M.; Sardar, N. Studies on Rheological Behavior of Xanthan Gum Solutions in Presence of Additives. *Pet Petrochem. Eng. J.* **2018**, *2*, 000165.
31. Jha, P.K.; Mahto, V.; Saxena, V.K. Study the Effect of Polymers on the Stability and Rheological Properties of Oil-in-Water (O/W) Pickering Emulsion Muds. *Korea-Aust. Rheol. J.* **2018**, *30*, 127–136. [[CrossRef](#)]
32. Jha, P.K.; Saxena, V.K.; Yatrājula, S.K.; Kumar, A. Impact of Natural Polymer (Xanthan Gum) and Bentonite Clay on the Development of Oil-In-Water (O/W) Emulsion Drilling Fluids. *Int. J. Innov. Technol. Explor. Eng.* **2021**, *10*, 129–136. [[CrossRef](#)]
33. Schramm, G. *A Practical Approach to Rheology and Rheometry*; Gebrueder Haake GmbH: Karlsruhe, Germany, 2000.
34. Ghannam, M.T.; Esmail, N. Rheological Properties of Carboxymethyl Cellulose. *J. Appl. Polym. Sci.* **1997**, *64*, 289–301. [[CrossRef](#)]
35. Pal, R. Viscoelastic Properties of Polymer-Thickened Oil-in-Water Emulsions. *Chem. Eng. Sci.* **1996**, *51*, 3299–3305. [[CrossRef](#)]
36. Sosa-Herrera, M.G.; Berli, C.L.A.; Martinez-Padilla, L.P. Physicochemical and Rheological Properties of Oil-in-Water Emulsions Prepared with Sodium Caseinate/Gellan Gum Mixtures. *Food Hydrocoll.* **2008**, *22*, 934–942. [[CrossRef](#)]
37. Chen, J.; Dickinson, E. Effect of Surface Character of Filler Particles on Rheology of Heat-Set Whey Protein Emulsion Gels. *Colloids Surf. B Biointerfaces* **1999**, *12*, 373–381. [[CrossRef](#)]
38. Nakamura, A.; Yoshida, R.; Maeda, H.; Furuta, H.; Corredig, M. Study of the Role of the Carbohydrate and Protein Moieties of Soy Soluble Polysaccharides in their Emulsifying Properties. *J. Agric. Food Chem.* **2004**, *52*, 5506–5512. [[CrossRef](#)]
39. Jin, Q.; Li, X.; Cai, Z.; Zhang, F.; Yadav, M.P.; Zhang, H. A Comparison of Corn Fiber Gum, Hydrophobically Modified Starch, Gum Arabic and Soybean Soluble Polysaccharide: Interfacial Dynamics, Viscoelastic Response at Oil/Water Interfaces and Emulsion Stabilization Mechanisms. *Food Hydrocoll.* **2017**, *70*, 329–344. [[CrossRef](#)]
40. Peng, F.; Xu, J.; Xu, H.; Bao, H. Electrostatic Interaction-Controlled Formation of Pickering Emulsion for Continuous Flow Catalysis. *ACS Appl. Mater. Interfaces* **2021**, *13*, 1872–1882. [[CrossRef](#)] [[PubMed](#)]
41. Shao, P.; Qiu, Q.; Chen, H.; Zhu, J.; Sun, P. Physicochemical Stability of Curcumin Emulsions Stabilized by *Ulva Fasciata* Polysaccharide under Different Metallic Ions. *Int. J. Biol. Macromol.* **2017**, *105*, 154–162. [[CrossRef](#)] [[PubMed](#)]
42. Jiang, Y.; Xu, Y.; Li, F.; Li, D.; Huang, Q. Pectin Extracted from Persimmon Peel: A Physicochemical Characterization and Emulsifying Properties Evaluation. *Food Hydrocoll.* **2020**, *101*, 105561. [[CrossRef](#)]

43. Akiyama, E.; Kashimoto, A.; Fukuda, K.; Hotta, H.; Suzuki, T.; Kitsuki, T. Thickening Properties and Emulsification Mechanisms of New Derivatives of Polysaccharides in Aqueous Solution. *J. Colloid Interface Sci.* **2005**, *282*, 448–457. [[CrossRef](#)] [[PubMed](#)]
44. Maleki, A.; Kjoniksen, A.L.; Nystrom, B. Effect of Shear on Intramolecular and Intermolecular Association during Cross-Linking of Hydroxyethylcellulose in Dilute Aqueous Solutions. *J. Phys. Chem. B* **2005**, *109*, 12329–12336. [[CrossRef](#)]
45. Bokyo, V.; Richter, S. Monitoring of the Gelation Process on a Radical Chain Cross-Linking Reaction Based on N-Vinylcaprolactam by Using Dynamic Light Scattering. *Macromol. Chem. Phys.* **2004**, *205*, 724–730. [[CrossRef](#)]